AGU PUBLICATIONS

Journal of Geophysical Research: Atmospheres

Supporting Information for

Contribution of the Southern Annular Mode on variations in water isotopes of daily precipitation at Dome Fuji, East Antarctica

K. Kino[1,2], A. Okazaki[3], A. Cauquoin[2], and K. Yoshimura[2]

[1]Atmosphere and Ocean Research Institute, The University of Tokyo, Kashiwa, Japan

[2]Institute of Industrial Science, The University of Tokyo, Kashiwa, Japan

[3]Hirosaki University, Hirosaki, Japan

Contents of this file

Introduction

To evaluate the simulated results, different datasets including isotopic measurements in precipitation, ice cores, and continental speleothems were used as in Cauquoin et al. (2019b) and compared with the simulation results (Figure S1). The observed $\delta^{18}O_p$ values were obtained from the Global Network for Isotopes in Precipitation (GNIP) observational database for at least five calendar years from 1961 to 2007 (IAEA/WMO, 2018). The ice core data are presented in Table 1 of Cauquoin et al. (2019). $\delta^{18}O$ in the calcite of speleothem was obtained from the Speleothem Isotope Synthesis and Analysis (SISAL) dataset (version 1b: Atsawawaranunt et al., 2019)updated by Comas-Bru et al. (2019). The speleothem values of $\delta^{18}O$ in calcite are converted to $\delta^{18}O$ in drip water as in Cauquoin et al. (2019b) using ERA-40 reanalysis data (Kållberg et al., 2004) and method of Tremaine et al. (2011). The simulated $\delta^{18}O_p$ was in very good agreement with present-day observations (Figure S1). The known features of the isotopic effects found by Dansgaard (1964) were well simulated, as confirmed by Okazaki & Yoshimura (2019), namely, enhanced depletion with latitude, altitude, and continentality.

Statistical analyses for the results of simulation (Figure 2 and Tables S1), and the results of in-situ observation at Dome Fuji (Fujita & Abe, 2006) were conducted (Table S2). While the number of samples was limited in Table S2, they supported most of the

features in Table S1. Standard deviations of modeled daily SAT and $\delta^{18}O_p$ in each month for the whole 1981-2010 period shown in Figure 3 are also summarized in Table S3.

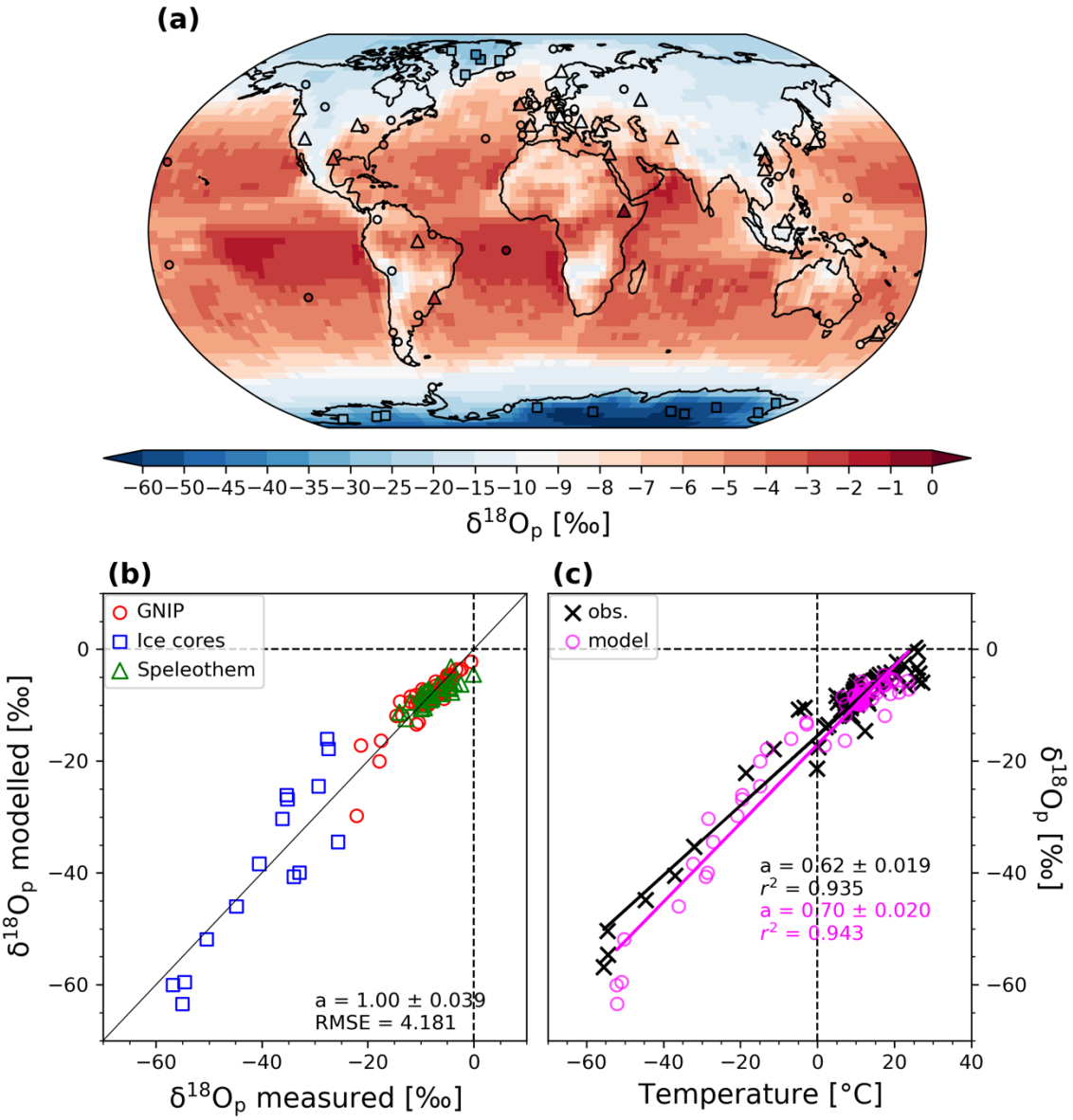

Figure S1 a Global climatological distribution of simulated (background pattern) and observed (colored markers; see text for details) annual mean $\delta^{18}O$ values in precipitation. The data consist of 70 GNIP stations (circles), 15 ice core records (squares), and 33 speleothem records (triangles). **b** Modeled vs. observed annual mean $\delta^{18}O_p$ at the different GNIP, speleothem, and ice core sites. **c** Observed (black crosses) and modeled (magenta circles) spatial $\delta^{18}O_p$ -surface air temperature relationship. The linear fits for the observed and modeled values are drawn as black and magenta lines, respectively. For both **b** and **c**, the gradients of the linear regression fits are expressed in each panel.

Table S1 Spearman's correlation coefficients and p-values between modeled daily $\delta^{18}O_p$ and surface air temperature (R_{SAT} and p_{SAT}), precipitation (R_{Pr} and p_{Pr}), and SAM index (R_{SAM} and p_{SAM}) in each month. Only correlation coefficients with p-values lower than 0.05 are shown (NaN if not). The number of effective days used for the analysis over the period 1981-2010 was also shown for respective months.

	Jan	**Feb**	**Mar**	**Apr**	**May**	**Jun**	**Jul**	**Aug**	**Sep**	**Oct**	**Nov**	**Dec**
Number of days	930	847	930	900	930	900	930	930	896	858	893	930
R_{SAT}	-0.29	0.14	0.45	0.43	0.49	0.55	0.57	0.51	0.46	0.45	NaN	-0.19
p_{SAT}	1.63E-19	6.91E-05	1.58E-48	2.10E-42	1.63E-56	7.42E-73	1.19E-79	1.98E-62	2.88E-48	8.32E-44	5.80E-01	2.65E-09
R_{Pr}	-0.53	-0.23	0.41	0.56	0.45	0.49	0.47	0.42	0.47	0.27	-0.39	-0.56
p_{Pr}	2.18E-67	1.93E-11	5.69E-39	9.82E-76	2.36E-48	1.46E-56	6.64E-52	1.10E-40	1.20E-49	1.71E-15	2.81E-33	2.09E-78
R_{SAM}	NaN	-0.13	-0.18	-0.18	-0.29	-0.36	-0.49	-0.40	-0.34	-0.34	-0.22	-0.10
p_{SAM}	1.09E-01	2.14E-04	6.25E-08	5.46E-08	5.98E-19	4.95E-29	6.25E-58	8.42E-38	1.57E-25	5.13E-25	1.20E-11	3.73E-03

Table S2 Same as Table S1 but for observation at Dome Fuji (Fujita & Abe, 2006) and the Japanese 25-year reanalysis fields (Onogi et al., 2007). The number of sampled days were also shown for respective months.

	Jan	**Feb**	**Mar**	**Apr**	**May**	**Jun**	**Jul**	**Aug**	**Sep**	**Oct**	**Nov**	**Dec**
Number of days	18	23	31	29	31	30	29	31	29	30	26	26
R_{SAT}	0.65	0.56	0.47	0.40	NaN	0.46	0.60	0.57	0.44	0.66	0.82	NaN
p_{SAT}	3.70E-03	5.94E-03	7.15E-03	3.13E-02	7.66E-01	1.02E-02	5.29E-04	8.83E-04	1.72E-02	8.03E-05	2.92E-07	6.26E-02
R_{Pr}	NaN	NaN	NaN	0.43	0.59	0.77	0.73	0.59	0.46	NaN	NaN	NaN
p_{Pr}	5.02E-01	1.05E-01	5.97E-01	1.97E-02	4.91E-04	5.29E-07	7.17E-06	5.10E-04	1.26E-02	3.27E-01	9.02E-02	3.44E-01
R_{SAM}	NaN	NaN	-0.57	NaN	NaN	NaN	NaN	NaN	-0.51	NaN	-0.57	NaN
p_{SAM}	2.91E-01	6.71E-02	7.54E-04	5.62E-01	6.48E-01	1.26E-01	1.03E-01	1.64E-01	4.82E-03	2.04E-01	2.17E-03	1.35E-01

Table S3 Standard deviations of modeled daily SAT and $\delta^{18}O_p$ in each month.

	Jan	**Feb**	**Mar**	**Apr**	**May**	**Jun**	**Jul**	**Aug**	**Sep**	**Oct**	**Nov**	**Dec**
SAT [°C]	2.78	4.47	5.72	6.84	8.24	8.45	8.57	7.41	6.97	6.09	4.51	2.77
$\delta^{18}O_p$ [‰]	7.08	9.39	10.11	11.63	13.69	13.65	14.89	13.70	13.56	14.25	10.55	7.35